



Developing parameter estimation techniques for controller optimization of a Coastal Profiling Float

Nicholas Sohn, Swarthmore College

Mentor: Gene Massion

Summer 2013

Keywords: Coastal Profiling Float, buoyancy engine, added mass, drag coefficient

ABSTRACT:

Several tools were developed to improve a theoretical model for optimizing the depth controller used in a Coastal Profiling Float. A laboratory apparatus for simulating high-pressure effects on a buoyancy engine was designed to withstand pressures up to 750 psi. Several efficiency metrics were outlined and measured using this benchtop prototype of the engine. Finally, a test procedure and software tools were developed for simultaneous measurement of the added mass and drag coefficient of a prototype float.

INTRODUCTION:

A full understanding of the ocean climate requires quantitative data with a level of temporal and geographic resolution that would be impractical to achieve using conventional ocean measurement systems. The Argo program introduced an alternative method for large scale measurement of heat exchange in the ocean using a network of autonomous profiling floats distributed on a global scale. Since the first deployment of Argo floats in 2000 over 3 500 new floats have been deployed by organizations spanning across 23 countries. The success of the program is emphasized by the fact that currently over 100 oceanographic research papers per year cite Argo data.

Despite the large amount of data that have become available in the ocean because of Argo floats, coastal waters have largely been avoided as sites for float deployments. Shallow waters and the proximity to the shore pose significant dangers to profiling floats that make coastal

deployments impractical, especially considering the low heat content in these environments. While coastal settings may not have a significant role in heat exchange, studying coastal environments is critical for understanding ocean acidification, hypoxia, and other effects that could potentially result from anthropogenic waste. A series of ocean floats modified for deployment in coastal waters could provide a cost efficient method of quantifying these changes.

The largest challenge associated with using floats for coastal measurements is containing the floats within the region of interest without significant human intervention. Coastal and tidal currents have the potential to push a profiling float into the coastline or further out to sea. Either of these scenarios would prevent a coastal float from collecting useful measurements. One solution is to program the floats to attach themselves to a substrate on the sea floor until they collect data. This would reduce the risk of drifting and additionally minimize the potential for biofouling. Another possible solution would be to program the float to change its depth and take advantage of serendipitous currents that would push the float to a more desirable position. Both of these methods require significantly finer control and stronger lifting forces than an Argo float can achieve.

The purpose of this project is to aid in the design of a buoyancy engine for a Coastal Profiling Float (CPF) modified from the Argo float design. The primary goal is to redesign a pressure simulator for characterizing the buoyancy engine at different depths. Additionally, this project seeks to refine the physical model of the float dynamics to inform the eventual design of a PID control loop for regulating float velocity and position. The remainder of this report is divided into sections describing the design of the pressure simulator, efficiency testing of the ballast engine, and system characterization of the test tank prototype.

PRESSURE SIMULATOR DESIGN:

During a single profiling measurement a CPF must travel through the water column starting at a depth anywhere between 100m and 50m underwater and travel at a constant velocity to the surface. As a result, the float is exposed to pressures ranging from around 15 psi at the surface 700 psi at depth. Varying pressure has a number of effects on the float including volume change from compression and the pressure head acting against the float's external bellows used for ballasting. Consequently, the external pressure on the float influences the pump efficiency. Before testing could be performed the pressure housing for the simulator had to be modified to withstand larger pressures. The first phase of this project was to quickly design and fabricate a

mechanism to secure the pressure housing lid with minimal modifications to the existing system, shown schematically in Figure 1 below.

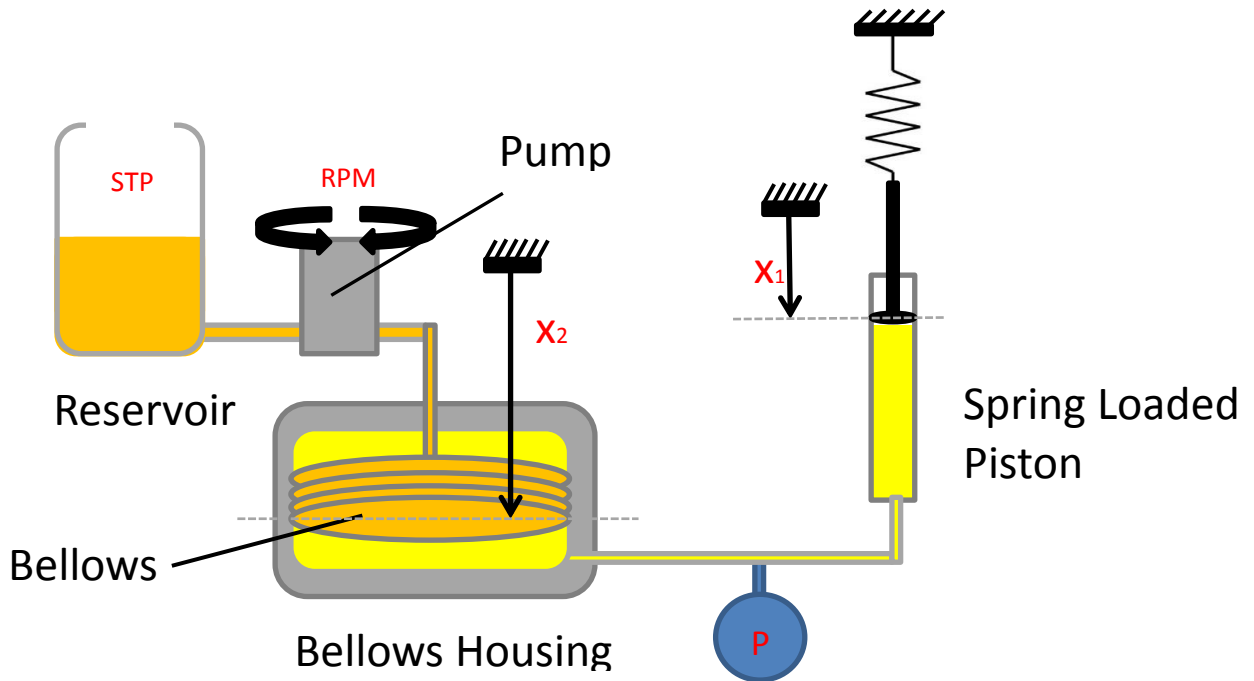


Figure 1 – The above schematic shows the setup for the pressure simulating apparatus. Measured variables are indicated in red.

Hydraulic fluid is pumped from a reservoir kept at atmospheric pressure to the bellows, which is housed within an aluminum drum. The housing is flooded with hydraulic fluid, which may pass to a spring loaded piston. The spring emulates the linear relationship between depth and pressure by providing an elastic force that resists piston displacement. As the bellows expands the piston must also expand to accommodate the added volume. This piston expansion causes the spring to compress, thereby increasing the pressure acting on the fluid. The simulated pressure can be measured using a pressure transducer in line with the piston, or by measuring the spring displacement. The bellows position and motor speed are also measured via a data acquisition system.

MODIFICATIONS TO THE PRESSURE HOUSING

The lid to the housing was originally secured using 16 ¼-20 bolts. These bolts had insufficient cross-sectional area to resist tensile loading, and excessive bolt elongation caused the

O-ring seal to fail. For a 90 durometer O-ring the limit for extrusion is 0.020 in.¹ The primary design requirement was to prevent the housing lid from exceeding this displacement limit. Time and ease of fabrication were also important considerations.

In the region of elastic deformation the extension of a material is proportional to the applied load and member length, and inversely proportional to the elastic modulus and cross-sectional area. The latter two of these sources of elongation were addressed. Sixteen 302 Stainless Steel C-clips placed around the perimeter of the bellows housing were chosen as the load bearing components, each of which had a throat width of 2.2 in and a thickness of 1.5 in, as indicated in Figure 2. This method increased the tensile area by a factor of 60, resulting in an overall elongation of .006 in at the O-ring gap.

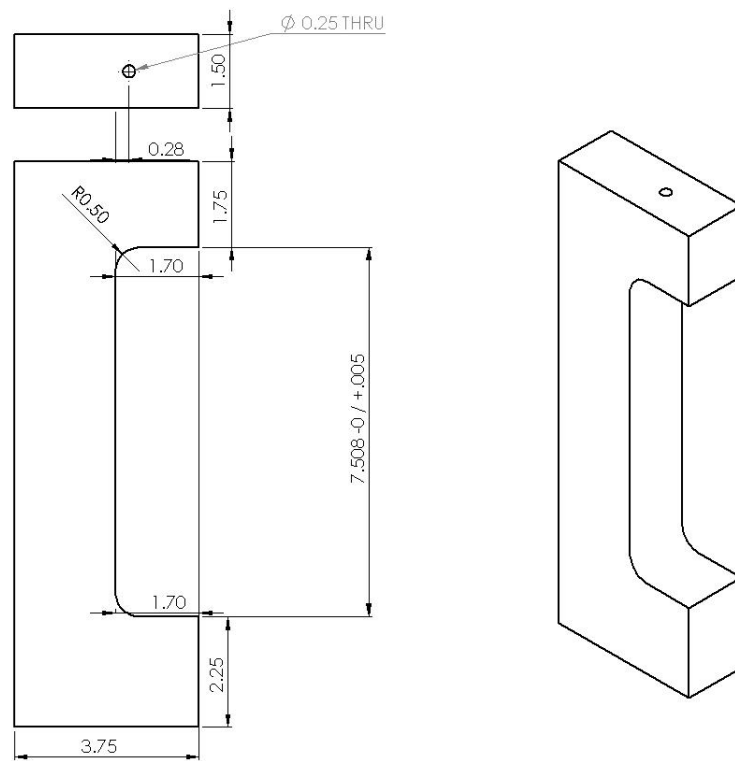


Figure 2 – The drawing above shows the dimensions and tolerances specified for the clips used to secure the pressure housing.

¹ Parker Hannifin Corp., 2007

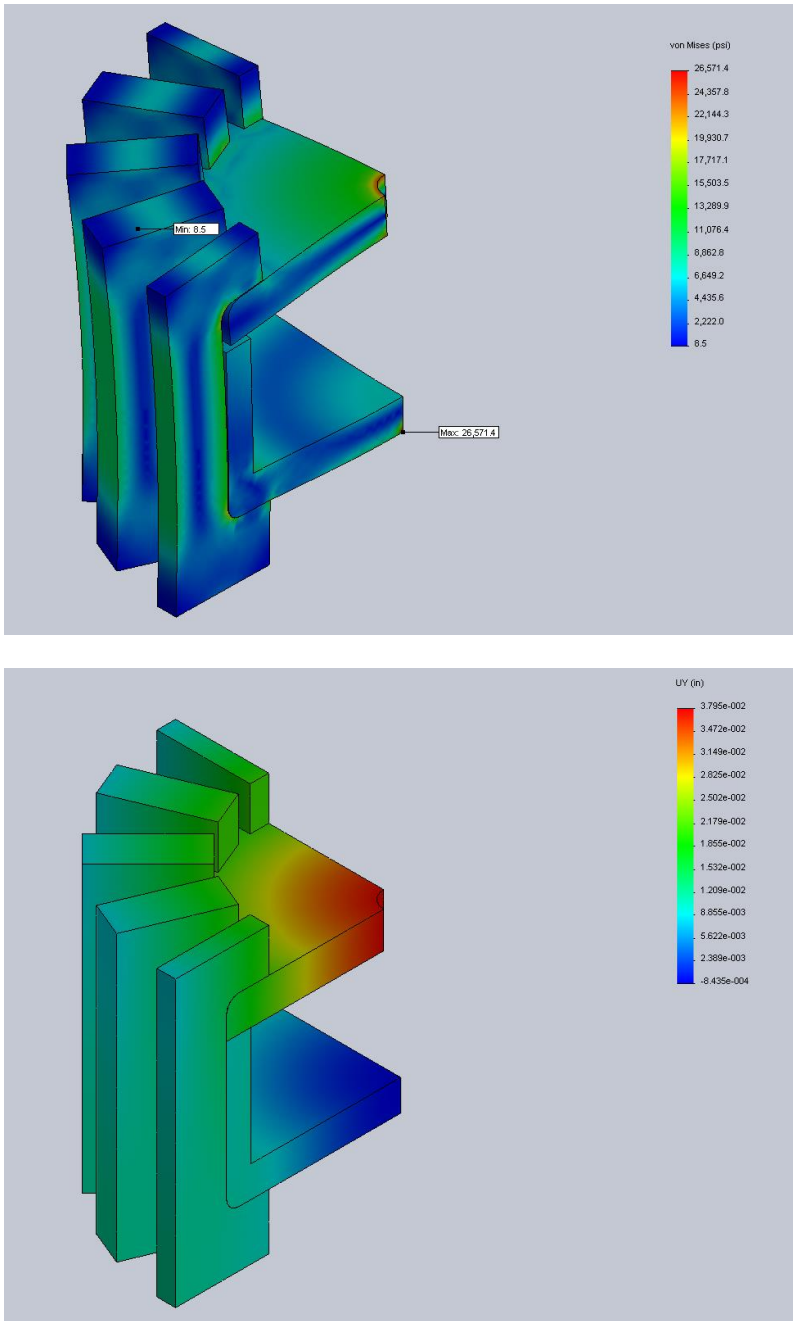


Figure 3 – The above plots indicate the von Mises stress and vertical displacement resulting from Finite Element Analysis. The maximum stress does not exceed the yield strength of Aluminum (40,000 psi). The displacement between the bellows housing an lid does not exceed the gap limit of .006 in.

A simple 90 degree cut into bar stock would be the simplest solution in terms of fabrication. However, the sharp corners of the inner face of the “C” caused unacceptably large stress concentrations. Finite Element Analysis (FEA) of the assembly results suggested that adding a 0.5 inch fillet to each corner would reduce the stress to an acceptable amount. In order to reduce

the amount of material required for each clip, the top and bottom edge of the bellows housing were also filleted to fit snugly against each clip. The FEA analysis of this solution is shown in Figure 3 below. Note that the maximum von Mises stress is 26 571psi, which is below the 30 000psi yield strength of 302 Stainless Steel. As expected, the bellows housing undergoes some deformation as a result of the high pressure. The surface between the bellows housing and lid however has a difference in vertical displacement of .006 in, which is less than the extrusion limit.

Such high magnitude pressures should also cause radial expansion of the housing, which could potentially dislodge the clips. A single bolt was run through the top of each clip into the ¼-20 tapped holes originally used to seal the housing. The FEA simulation in Figure 4 verified that the addition of alignment bolts did not significantly change the loading of the pressure vessel.

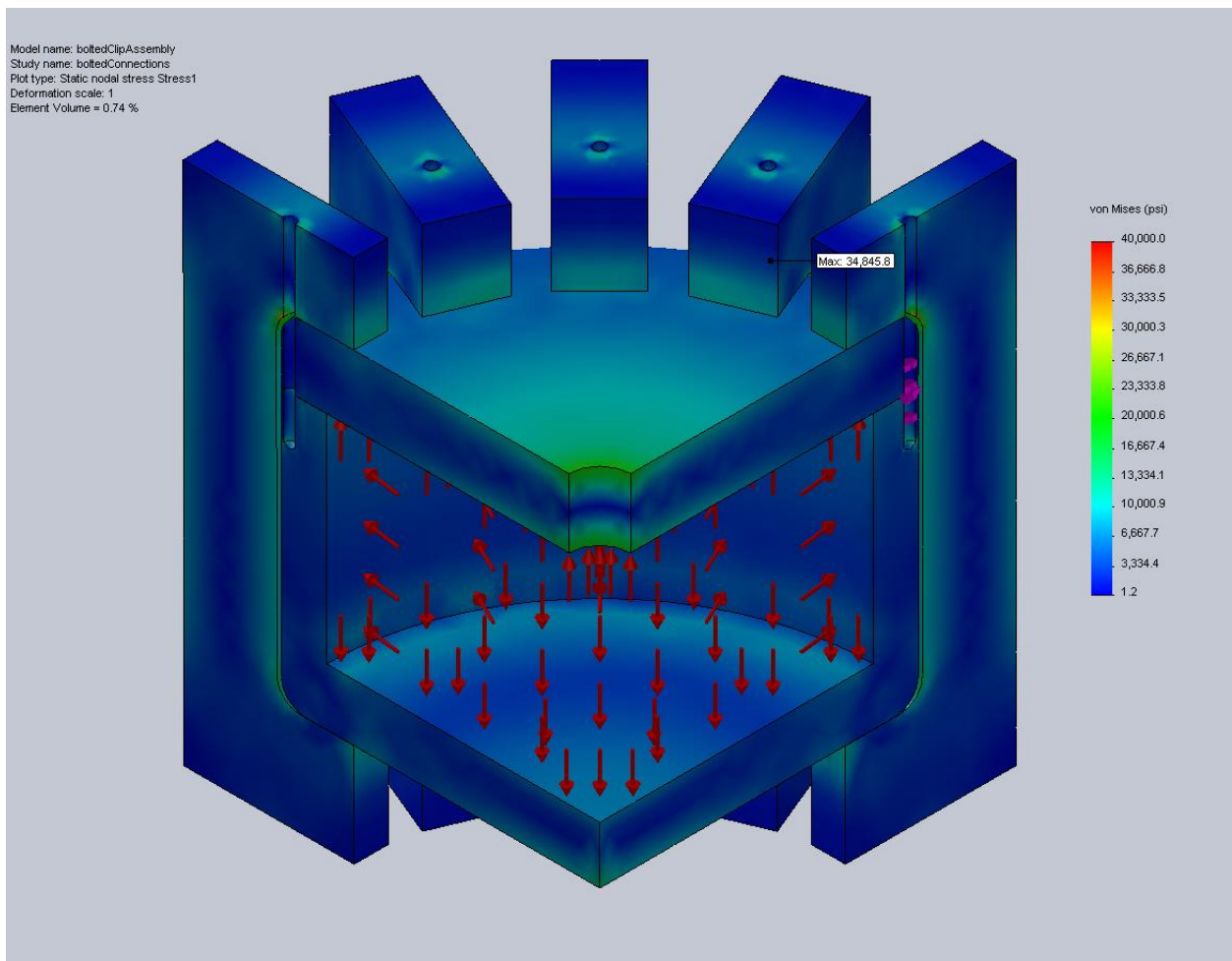


Figure 4 – The addition of bolts through the top each clip into the bellows housing does not significantly affect the stresses acting on the assembly

For the sake of clarity Figure 5 only indicates stresses greater than 20,000 psi. As expected, the point of maximum stress occurs at the junction between the C-clip and housing lid around the bolt clearance hole. Since the maximum stress is well below the yield strength of stainless steel this solution was chosen for the final design.

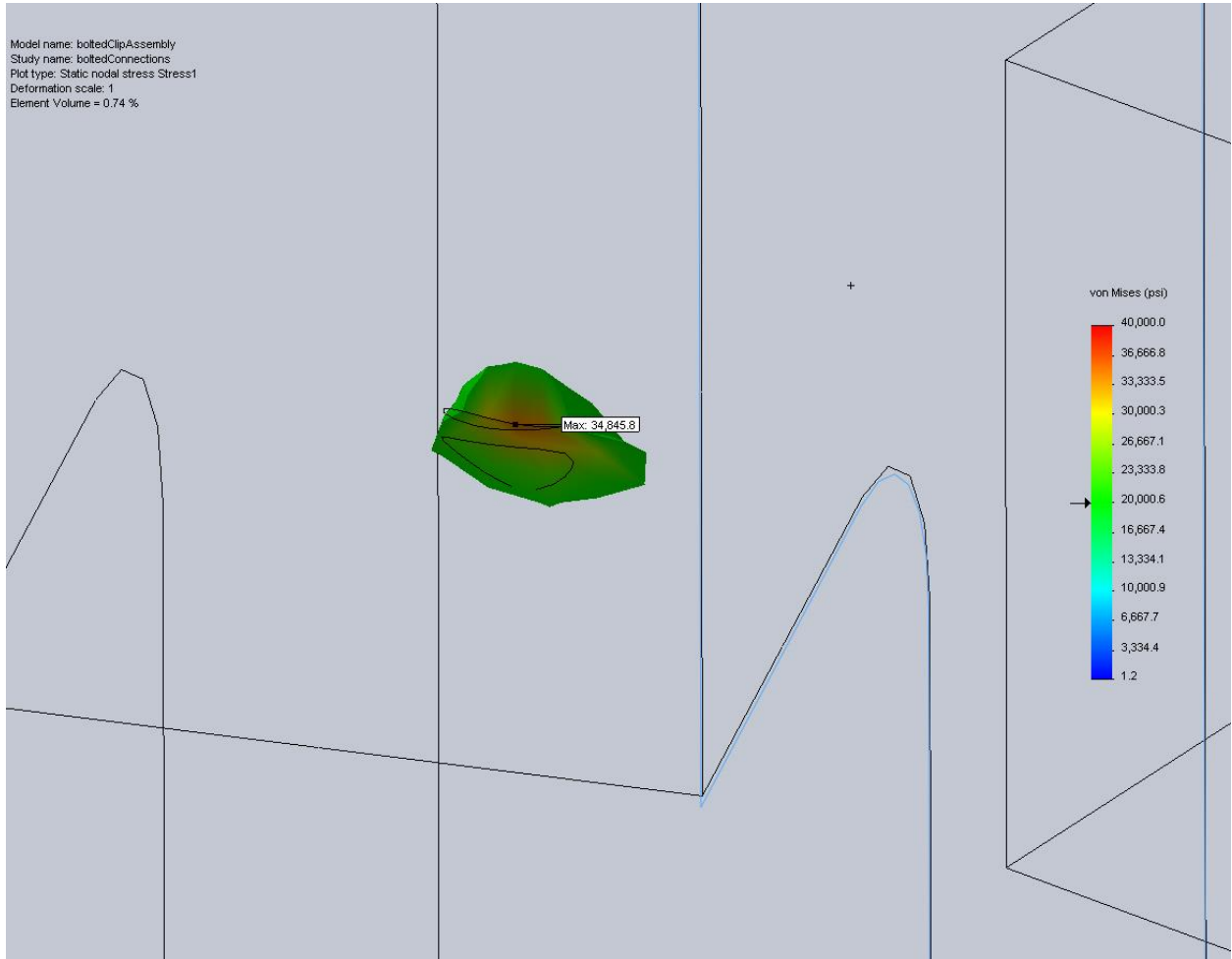


Figure 5 – The drawing above only indicates stressed above 20,000 psi. The maximum stress in the entire assembly is 34,845.8 psi.

HYDRAULIC ASSEMBLY

The design for the bellows engine on the CPF uses an Oildyne 865mL miniature piston pump to transport oil between the internal reservoir and external bellows. The hydraulic scheme depicted in Figure 6 below provides a path for oil to flow in each direction without back-flowing through the filters preceding pump inlets. Quarter inch Swagelok fittings were used for all pressurized lines. ClearFlex ¼ inch inner diameter PVC tubing was used for all low pressure lines. The motor, pump, and pilot valves were mounted to a frame fixed on the bellows housing.

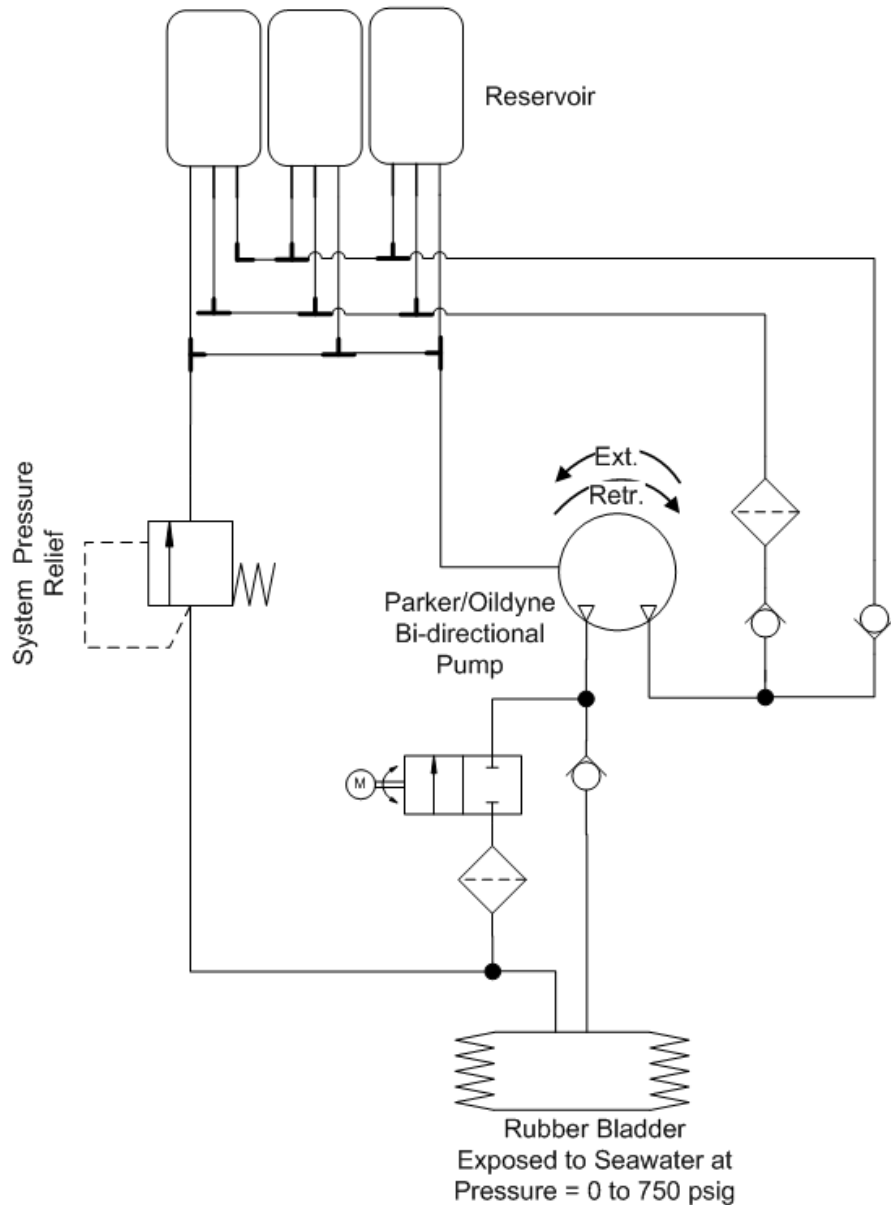


Figure 6 – The schematic above illustrates the hydraulic assembly used to pump oil from the reservoir to the external bladder and vice versa.

SENSOR AND DATA ACQUISITION MODULE INTEGRATION

The pressure simulator employs several commercial-off-the-shelf devices for acquiring engineering data. Two MTS position transducers record the vertical positions of the bellows and spring-loaded piston respectively. An OmegaDyne PX329-1KG5V transducer measures the pressure within the piston. Data from these devices are collected using a National Instruments cDAQ 9164. Analog data, including the voltage across a shunt resistor, are passed through a NI

cRIO-9215 analog input module. Digital data from the MTS position transducer must be extracted using a NI 9401 digital input module. The Maxon motor is controlled by an Elmo Harmonica, which receives feedback data from an incremental encoder. The wiring schematic used is shown in Figure 7 below:

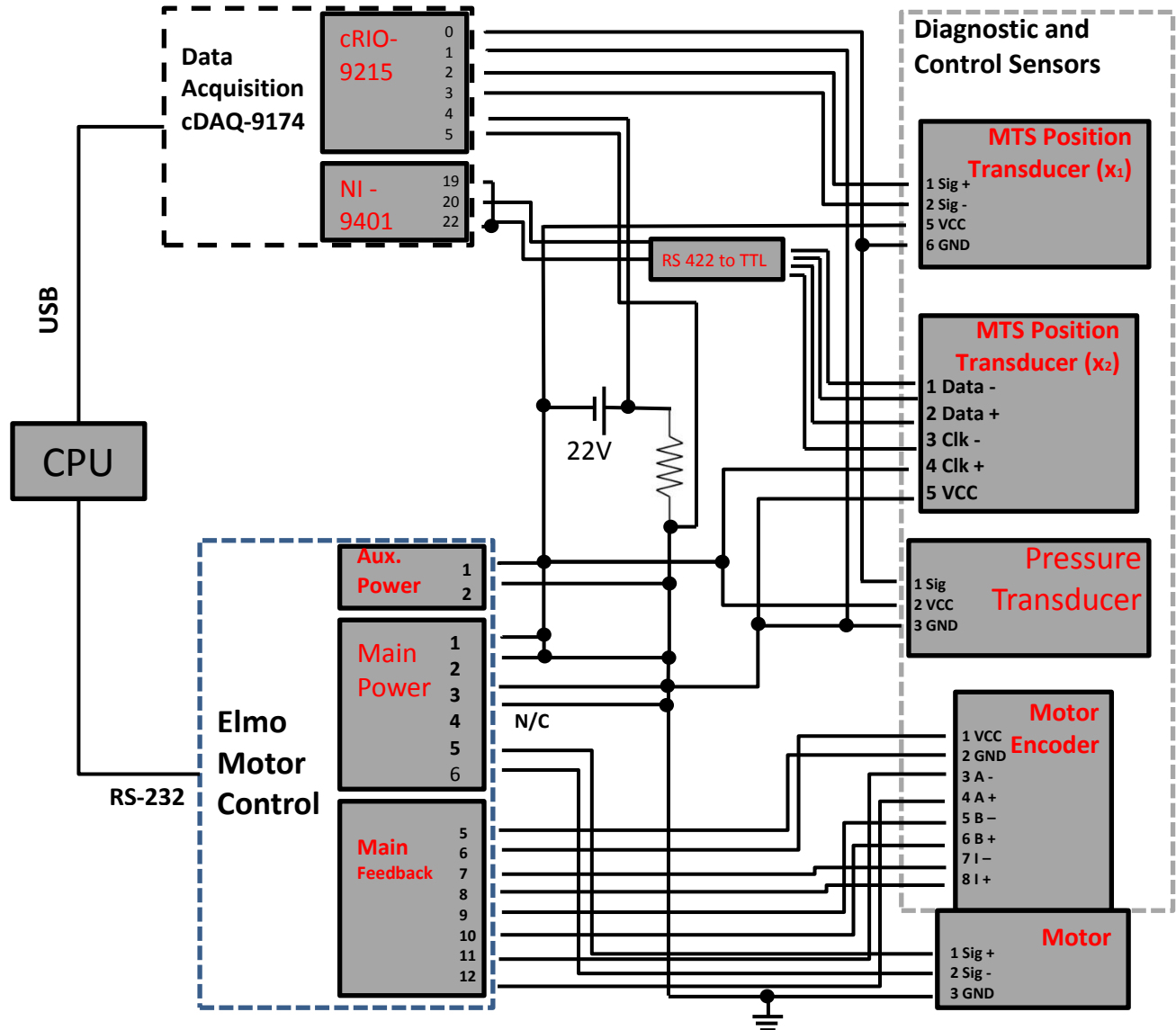


Figure 7 – The wiring diagram above reflects the organization of sensors and motor controller for the benchtop simulator.

PUMP EFFICIENCY TESTING

Pump efficiency was characterized using three metrics. The efficiency was measured as the bellows volume change per pump cycle and as the change of the product of volume and pressure

per Joule of electrical power supplied by the voltage supply. The latter metric was also measured for different bus voltages at a constant pressure.

Volumetric efficiency measurements



Figure 8 – The above sketch shows the idealized geometry of the bellows.

Flow rate into the bellows was determined by measuring the vertical displacement of the bellows endcap. Qualitative observation of the filling bellows indicated a specific filling order, which was modeled using a piecewise-nonlinear equation. The bellows, shown in Figure 8, can be broken into two cylinders with a radius (r_i) of 4.72 and height (c) of 0.2 in, four cylinders with a radius (r_o) of 5.91 in and height (d) of 0.08 in, and eight partial cones. The partial cones may be thought of as a series of stacked circular sections, whose radii vary as a function of height according to Equation 1 below, where h_{total} is the height of a single conic section.

$$r(h) = r_0 + \frac{r_i - r_o}{h_{total}} \cdot h \quad (\text{Eq. 1})$$

The cross-sectional area may also be expressed as a function of height as in Equation 2:

$$SA(h) = \pi \left(r_0 + \frac{r_i - r_o}{h_{total}} \cdot h \right)^2 \quad (\text{Eq. 2})$$

The volume at any given height for a partial conic section is therefore given by:

$$V(h) = \int_0^h \pi \left(r_0 + \frac{r_i - r_o}{h_{total}} \cdot h \right)^2 dh \quad (\text{Eq. 3})$$

Qualitative observations of the bellows filling suggested that the large cylindrical sections fill first, followed by the conic sections, and finally by the small cylindrical sections. The final piece-wise equation used to relate the bellows height to the volume is given below:

$$V(h) = \pi r_0^2 h * U(h) + 8 \left[\frac{\pi m^2 h_1^3}{3} + \frac{2\pi m b h_1^2}{2} + \pi b^2 h_1 \right] * U(h - 4d) + \pi r_i^2 h_2 * U(h - 4d - 8h_{total}) \quad (\text{Eq. 4})$$

Equation 4 defines U(h) as the step function and h₁ and h₂ are defined as:

$$h_1 = \frac{h - 4d}{8} \quad (\text{Eq. 5})$$

$$h_2 = h - 4d - 8h_{total} \quad (\text{Eq. 6})$$

The volumetric efficiency was measured by dividing the volume change calculated using Eq. 4 by the theoretical input flow rate. The input flow per pump revolution was assumed to be a constant 0.692 mL per revolution. The input flow could then be determined by multiplying this constant by the motor speed.

ENERGY EFFICIENCY MEASUREMENTS

Pump efficiency was also characterized in terms of work. The input work was measured from the current through a shunt resistor (0.05 Ω), using the equation $P = I^2 R$. The output work was calculated by multiplying the bellows pressure by the change in bellows volume.

EXPERIMENTAL DESIGN

Efficiency v. Pressure

Prior to the experiment all hydraulic fluid was evacuated from the bellows and the pressure inside the bellows housing was measured. The pump was then driven at a rate of 100 rpm until the vessel reached a pressure of 250psi. The resulting pump efficiency was plotted as a function of pressure using both energy and volumetric methods. This process was repeated twice over a range of pump speeds from 100rpm to 5 000rpm. Figure 9 and Figure 10 show two sample trials using a motor speed of 500rpm. These results indicate good repeatability between trials. Note that Figure 9 indicates a steep drop in efficiency as the pressure drops to 0, whereas Figure 10 shows a more gradual decrease. The sharp drop in the volumetric efficiency does not seem accurate, and there are several factors that could create this error. The first is that when the

bellows is nearly empty the bellows velocity is a poor indication of the volume change. Furthermore, qualitative observations indicate that the pressure simulator has a small amount of air trapped in the spring loaded cylinder, which creates some compressibility. Both of these factors would be relevant only for small pressures, and can therefore be safely ignored in a full scale test.

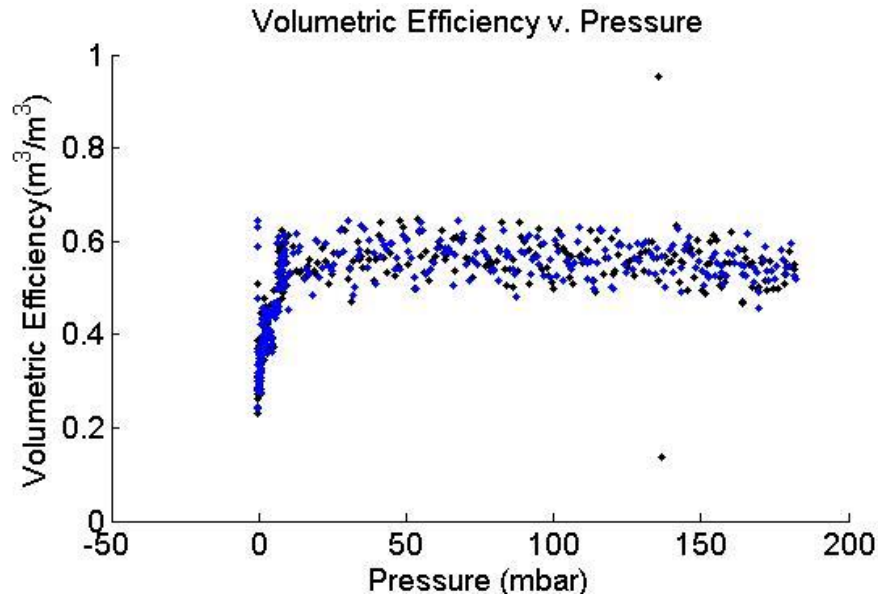


Figure 9 - The above plot shows two trials measuring volumetric efficiency at a motor speed of 500rpm. The first trial is plotted in black, and the second trial is plotted in blue.

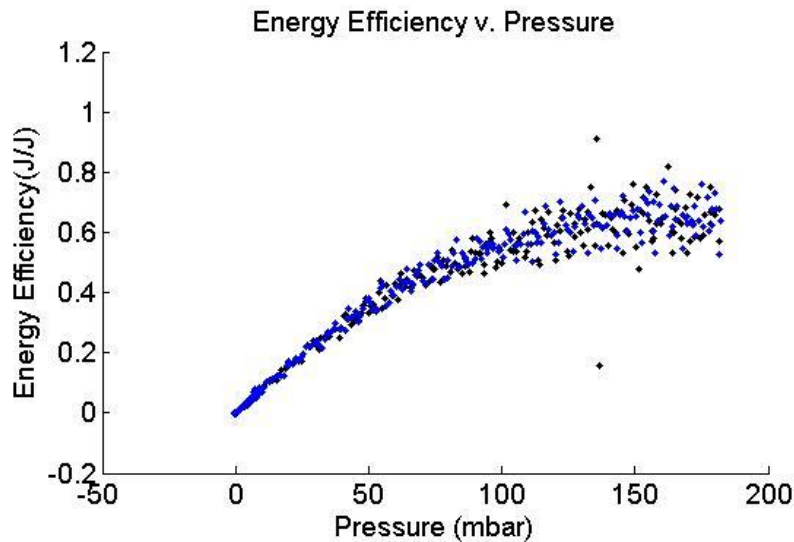


Figure 10 - The above plot shows two trials measuring energy efficiency at a motor speed of 500rpm. The first trial is plotted in black; the second trial is plotted in blue.

Energy Efficiency v. Bus Voltage

Prior to the experiment all hydraulic fluid was evacuated from the bellows and the pressure inside the bellows housing was measured. The pump was then driven at a rate of 500 rpm until the vessel reached a pressure of 250 psi. This process was repeated twice over a range of bus voltages from 22V to 24V in 0.5V increments. These results are shown in Figure 11 and Figure 12 below. Perhaps due to the small change in bus voltage, neither metric of efficiency shows strong sensitivity to the voltage change.

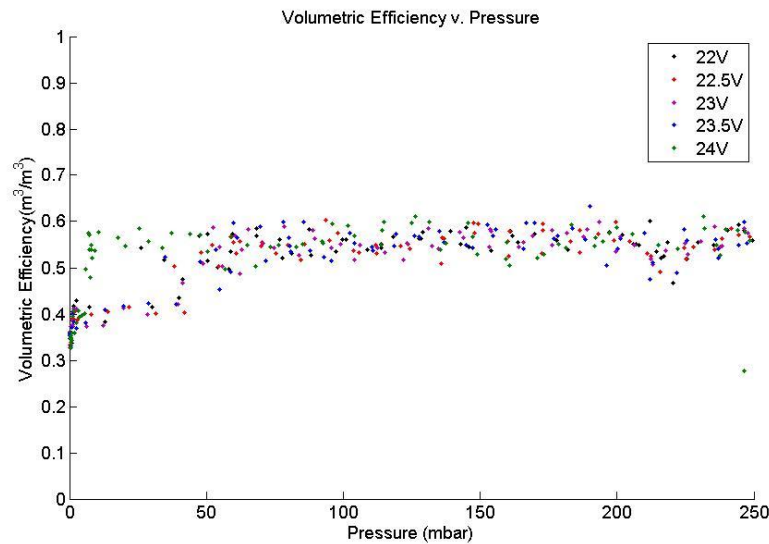


Figure 11 – The above plot shows volumetric efficiency as a function of pressure for different bus voltages.

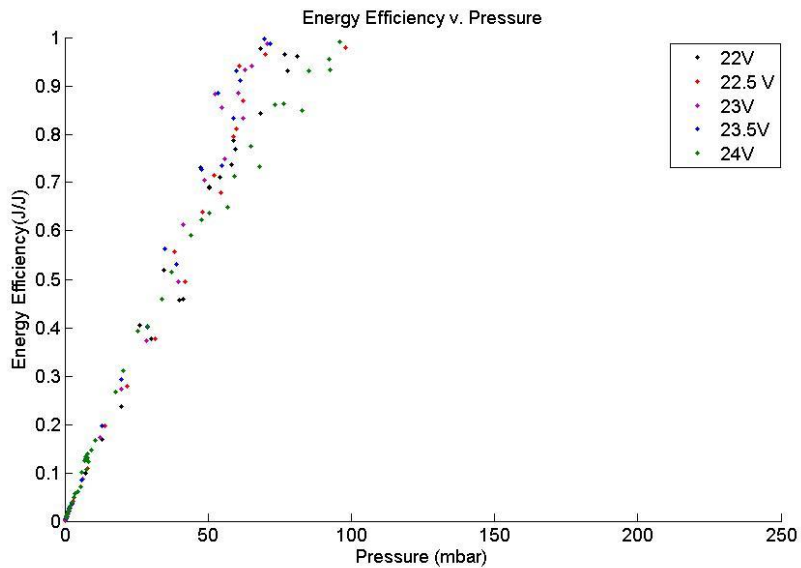


Figure 12 - The above plot shows energy efficiency as a function of pressure for different bus voltages.

SYSTEM CHARACTERIZATION OF TEST TANK FLOAT

The drag force is commonly approximated using the empirical equation²

$$F_{drag} = \frac{C_d v^2 A}{2} \quad (\text{Eq. 7})$$

where C_d is an empirical constant known as the drag coefficient. The drag coefficient varies with the object's shape, direction of flow, and the Reynolds number. The drag coefficient at the velocities a profiling float would typically experience is irrelatively insensitive to changes in the Reynolds number, therefore only effects of the direction of flow are important. Under ideal conditions the drag coefficient could be calculated from Eq. 7 by weighting the float with a known force and measuring its terminal velocity. Without writing a control loop to control bellows position however, the bellows will compress as the pressure increases beneath the surface, which decreases the buoyant force acting on the float. Since terminal velocity could not be achieved, a steady state measurement could not be used and acceleration also needed to be considered. The drag coefficient and added mass therefore needed to be determined simultaneously. The following procedure was only applied to measure the drag coefficient in descent, but could easily be modified to measure the drag coefficient during ascent.

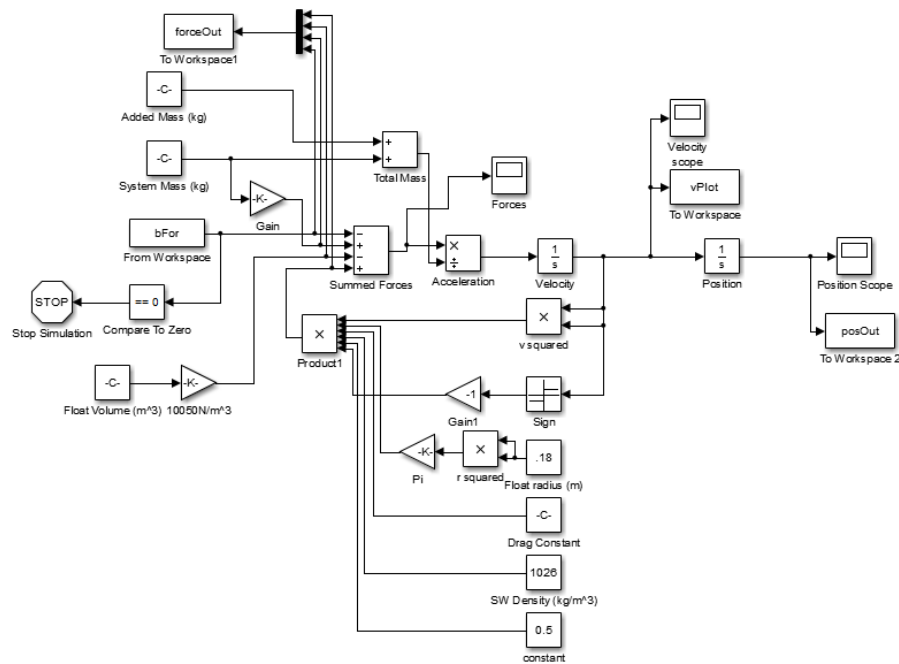


Figure 13 - The above Simulink model was created to simulate the physics of the added mass tests.

² Roberson and Crowe, 1993

A test tank prototype of the CPF was pre-ballasted to a known weight and released from the surface. The pressure data and bellows position were recorded over time. These results were compared to a numerical simulation where the drag coefficient and added mass could be varied independently. The Simulink model shown in Figure 13 was run iteratively varying each of these variables independently. The sum of the squared error was assigned to each combination of drag coefficient and added mass, which was plotted in a 2D error map. Error maps from different trials were combined by multiplying corresponding error values from each test, and raising the product to one over the number of elements combined. The resulting error map is shown in Figure 14. The drag coefficient and added mass estimates that gave the lowest error were inputted into each simulation, resulting in the float trajectories plotted in Figure 15. Note that the results for the float pre-ballasted to 7.5g shows poor agreement between the predicted and actual trajectory. This is most likely due to an error in the initial measurement of the system mass. This assumption is based on Figure 15, which indicates that none of the predicted trajectories matched the actual trajectory very well. However, the close agreement between the other two trajectories suggests that with more precise measurements of the system this procedure could be a viable means of determining the drag coefficient and added mass simultaneously.

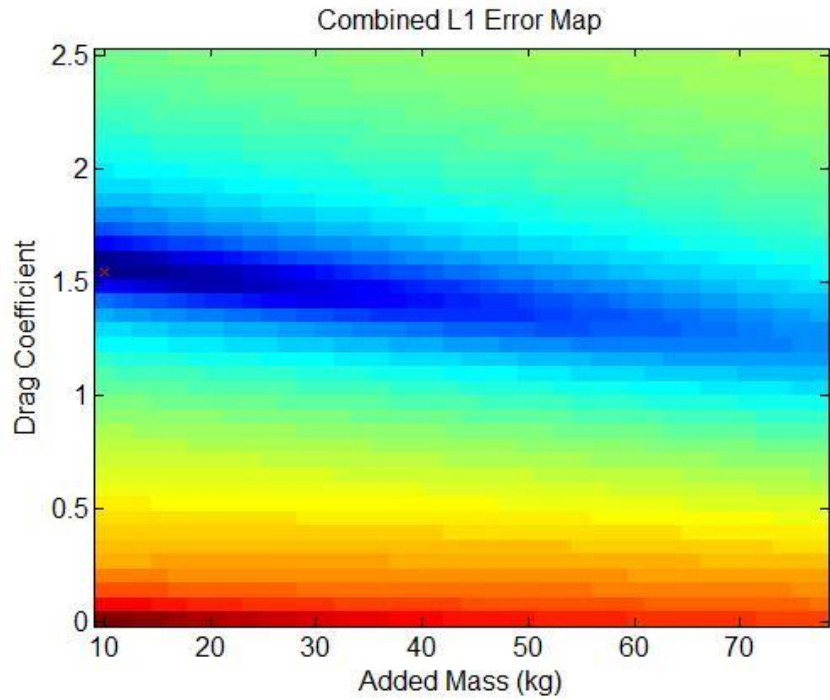


Figure 14 – The plot above shows the Combined Error Map resulting from 2D Least Square Regressions applied to each trial.

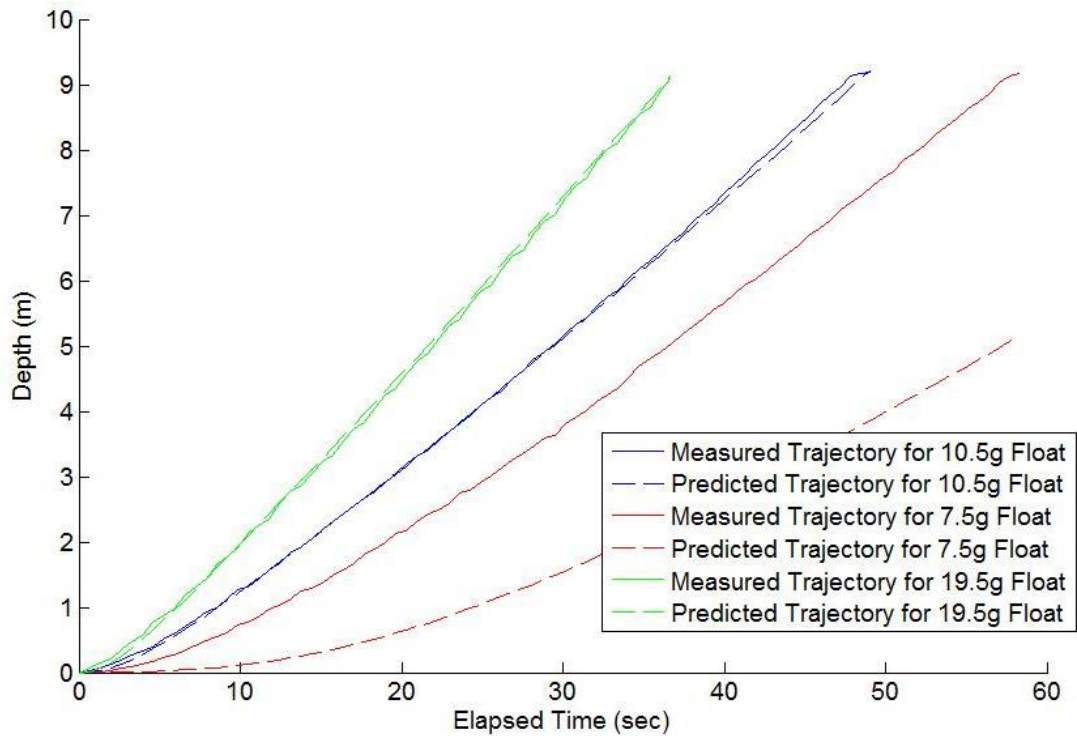


Figure 15 – The above plot compares predicted and measured trajectories for float ballasted to different set weights, as indicated by the line of the color. Predicted trajectories are dotted, measured trajectories are continuous lines.

CONCLUSION

This completion of this project resulted in several advancements for the Coastal Profiling Float project. The largest accomplishment of the project was the completion of a fully operation pressure simulator for the buoyancy engine. The pressure simulator was complemented by the development of software tools and a procedure for characterizing the engine performance at high pressures. This characterization is critical to developing a better depth controller. This project also addressed other aspects of float hydrodynamics, which further informs the theoretical model. The procedure for simultaneous measurement of added mass and drag coefficients enables simple measurements without introducing errors that may result from a bellows-position based controller. The methods for parameter estimation performed on the test tank prototype can easily be applied to a sea-going or any future prototype. While there will undoubtedly be other complications with the sea-going model, this project provides a strong starting point for eventually optimizing its depth controller.

ACKNOWLEDGMENTS

This research would not have been possible without the support of the Monterey Bay Aquarium Research Institute and The David and Lucile Packard Foundation. Gene Massion provided invaluable insight and guidance and helped shape this project. Mike Parker fabricated many of the components in the test apparatus. The contributions of Ken Johnson, Carole Sakamoto, Ginger Elrod, Patrick Gibson, Jose Rosal and Frank Flores are also noted.

REFERENCES

- Parker Hannifin Corporation. Parker O-Ring Handbook. Cleveland: Parker Hannifin Corp., 2007
- Roberson J.A. and C.T. Crowe. *Engineering Fluid Mechanics*. New York: John Wiley & Sons, Inc., 1993